J Fluoresc (2017) 27:2239–2251
DOI 10.1007/s10895-017-2166-3

ORIGINAL ARTICLE

Transition Metal (II) Complexes with a Novel Azo-azomethine Schiff Base Ligand: Synthesis, Structural and Spectroscopic Characterization, Thermal Properties and Biological Applications

Gökhan Yeğiner[1] · Mehmet Gülcan[1] · Sema Işık[2] · Gülsiye Öztürk Ürüt[2,3] · Sadin Özdemir[4] · Mükerrem Kurtoğlu[5]

Received: 21 April 2017 / Accepted: 10 August 2017 / Published online: 24 August 2017

Abstract The pyrimidine based azo-linked Schiff base ligand, 5-benzoyl-1-((E)-(2-hydroxy-3-methoxy-5-((E)phenyldiazenyl) benzylidene)amino)-4-phenylpyrimidin-2(1H)-one (HL), and its transition metal (II) complexes were synthesized and defined by using ^{1}H-NMR, ^{13}C-NMR, Elemental analysis, FT-IR, MS, UV–vis, molar conductance, magnetic susceptibility and thermal analysis techniques. According to the conductance data obtained indicate all of the metal complexes have non-electrolytic nature. Square pyramidal geometry for Pd(II) and octahedral geometry for all the other complexes synthesized was concluded from the electronic absorption spectra and magnetic susceptibility measurements of the complexes. Investigation of the significant infrared bands of the active groups in the ligand and the solid complexes alludes that HL is coordinated to the metal ions ONO tridentate manner. Moreover, the absorption and emission properties of the azo-azomethine based ligand and its complexes were investigated. The results obtained show that fluorescence emissions of the ligand and its metal (II) complexes depend on the type of transition metal ions and the derivatives displayed moderate Stokes' shift values between 44 and 107 nm. All the compounds exhibited superb photostability. Further, antioxidant, antimicrobial and pBR322 plasmid DNA cleavage activities were investigated. All compounds showed good DPPH• (1,1-diphenyl-2-picrylhydrazyl) radical scavenging activity and complexes of $[MnL_2]\bullet H_2O$ and $[NiL_2]\bullet H_2O$ exhibited excellent metal chelating activity. All the compounds tested demonstrated two strand DNA cleavage activities.

Keywords Azo-azomethine · Transition metal complex · Fluorescence · Biological application

Introduction

The condensation of primary amines with carbonyl compounds produces Schiff bases which were named after Hugo Schiff in 1864 [1]. These compounds common structural property is the azomethine group which has a general formula of R-HC=N-R. Schiff bases are used as ligands in the coordination chemistry. These ligands and their transition metal complexes have increased extremely and comprise an extensive field of organometallic compounds and diverse appearance of bioinorganic chemistry. Schiff base ligands were studied to exhibit different biological actions by merit of the azomethine linkage, which gives opportunity for many applications like antibacterial, antifungal and analytical activities [2–5]. On the other hand, metal complexes with oxygen and nitrogen donor Schiff bases gain special concern, due to their capability to have unusual geometry [3, 6–9].

Azo dyes are one of the significant classes of organic colorants, which consist of at least a conjugated azo (-N=N-)

Electronic supplementary material The online version of this article (doi:10.1007/s10895-017-2166-3) contains supplementary material, which is available to authorized users.

✉ Mehmet Gülcan
mehmetgulcan65@gmail.com

✉ Gülsiye Öztürk Ürüt
gulsiye.ozturk@deu.edu.tr; gulsiyeozturk@yahoo.com

[1] Department of Chemistry, Science Faculty, University of Van Yüzüncü Yıl, Van, Turkey

[2] Department of Chemistry, Science Faculty, University of Dokuz Eylül, Tınaztepe, Izmir, Turkey

[3] Department of Chemistry, Faculty of Sciences, Dokuz Eylül University, Tinaztepe Campus, 35160, Buca, Izmir, Turkey

[4] Food Processing Programme, Technical Science Vocational School, Mersin University, TR-33343, Yenisehir, Mersin, Turkey

[5] Department of Chemistry, Science Faculty, University of Kahramanmaraş Sütçü İmam, Kahramanmaraş, Turkey

chromophore, and are the major and most sophisticated class of dyes [10]. Owing to their effective physico-chemical properties azo compounds have gained substantial interest. These derivatives have been intensively investigated for nonlinear optics, optical information storage and switching [11]. In addition to them, azo-azomethines were broadly utilized as coloring matter for wool, synthetic fabrics and leather due to their remarkable dyeing features and also in components of optical communication systems, photonic devices and electro-optic modulators because of their second-order nonlinear optical features [12, 13].

In last years the research for new organic stuff which is applicable in light emitting devices has gained considerable interest [14–17]. For instance, especially blue region emitting organic polymers at low driving voltages are very interesting for flat panel display applications [18, 19]. Besides, rare earth complexes with low molecular weight organic ligands were also investigated to produce materials with high fluorescence for electroluminescent instruments [20, 21] and laser framework [22]. Additionally, many aromatic amines and polymeric arylamines were prepared as hole transport layers in organic electroluminescent investigation.

Oxygen is essential for the aerobic organisms to survive. Unfortunately, various reactive oxygen species (ROS) such as hydrogen peroxide, superoxide anions, nitric oxide and hydroxyl radicals occurs in the course of the oxygen metabolism. These free radicals must be reduced as they have toxic effects on cells and tissues. Antioxidant agents play an important role in the prevention of human diseases by free radical mediated toxicity [23]. A new trend in the area of antioxidant improvement focuses on multipotent antioxidant substances that can avoid biological organisms from oxidative damage. However, these synthesized antioxidant substances should have no toxic effects. For this reason, there is a growing demand and concern for safer antioxidants in pharmaceutical and food applications. On the other hand, there is also an increasing interest in developing new compounds that can interact with DNA for application in chemotherapy. These compounds, specifically their metal complexes can be also used as chemotherapeutic agents to cure a diversity of illnesses such as AIDS, cancer etc. These metal complexes can interact with DNA duplex through a diversity of binding modes including DNA intercalation, covalent and non-covalent binding and DNA cleavage [23, 24].

From perspective of the above-mentioned inquiry and the sustained concern to coordination compounds, the present work deals with the synthesis and features of a new azo-azomethine based fluorescent dye having ONO donor set of atoms obtained by the condensation reaction of *N*-Aminopyrimidine-2-one with 2-hydroxy-3-methoxy-5-(phenyldiazenyl)benzaldehyde, along with its metal(II) complexes (Schemes 1 and 2). The newly prepared compounds were characterized by structurally. Thermal properties of the prepared azo-linked Schiff base ligand and its metal(II) complexes have been further investigated by thermal analysis techniques. Moreover, fluorescent properties of azo-azomethine dye and its metal(II) complexes were examined. Also, the free radical scavenging features of the derivatives have been rated by using diverse methods, such as the DPPH• scavenging activity, metal chelating assay and reducing power and were evaluated. In addition, antimicrobial and pBR322 plasmid DNA cleavage activities were investigated.

Experimental

Materials and Instrumentation

All of chemicals utilized in this work were purchased from Aldrich or Merck and used without any purification. Solvents used for the synthesis were purified and dried by usual methods [25]. Elemental analyses (C, H, N and S) were performed on a Leco CHNS model 932 automatic elemental analyzer. FT-IR spectra were recorded on a Bio-Rad-Win-IR spectrophotometer applying KBr discs in the range of 4000–400 cm^{-1}. Electronic absorption spectra in the visible and ultraviolet regions were measured on a Shimadzu 1601 PC spectrophotometer (Tokyo, Japan). The magnetic susceptibility was determined with a magnetic susceptibility balance 436 Devon Park Drive (USA) using $Hg[Co(SCN)_4]$ as a calibrant. ^{1}H-NMR and ^{13}C-NMR spectra were carried out on a Bruker 300 MHz Ultrashield TM NMR instrument, using deuterated dimethyl sulfoxide ($DMSO\text{-}d_6$) as a solvent. All fluorescence measurements were undertaken by using Varian-Carry Eclipse spectrofluorimeter (Mulgrave, Australia). Thermogravimetric analysis (TG and DTG) and differential thermal analysis (DTA) experiments were performed using a SII Exstar TG/DTA 6300 in the temperature range 25–1000 °C with a heating rate of 40 °C min^{-1} under flowing nitrogen atmosphere (30 ml min^{-1}).

Synthesis of the Precursors

Azo-coupled salicylaldehyde precursor, 2-hydroxy-3-methoxy-5-(phenyldiazenyl)benzaldehyde [26, 27] and a pyrimidine-based primary amine derivative, *N*-aminopyrimidine-2-one [28], were synthesized by the well-known literature procedures.

Synthesis of the Azo-azomethine Based Ligand (HL)

The pyrimidine-based azo-azomethine ligand (HL) was prepared by 1:1 condensation reaction between 2-hydroxy-3-methoxy-5-(phenyldiazenyl)benzaldehyde and *N*-aminopyrimidine-2-one (Scheme 1). A hot anhydrous ethanolic solution of *N*-aminopyrimidine-2-one (1 mmol; 291 mg) and 2-hydroxy-3-methoxy-5-(phenyldiazenyl)benzaldehyde (1 mmol; 256 mg) was refluxed for 3 h. Then the hot mixture was filtered and the solid obtained was washed with hot ethanol (three times) and then with diethyl ether.

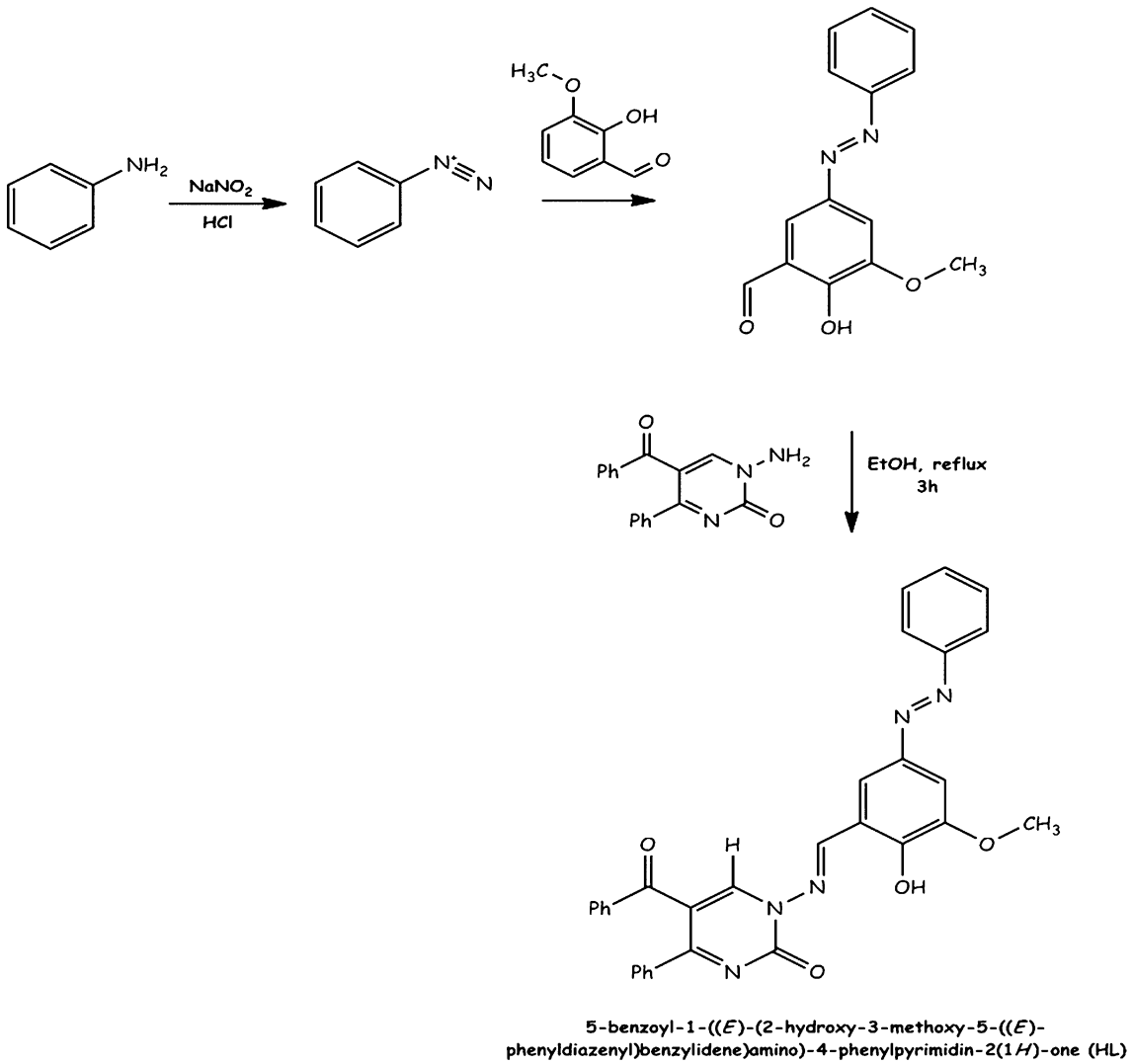

Scheme 1 Synthetic route of the ligand (HL)

Yellow powder, yield 79%, Mp 252 °C. Anal. Calc. for $C_{31}H_{23}N_5O_4$ (529.55 g/mol): C, 70.31; H, 4.38; N, 13.23. Found: C, 70.33; H, 4.32; N, 13.18%. FTIR data (KBr, cm^{-1}): 3433 ν(OH), 3054 ν(C-$H_{aromatic}$), 2970 ν(C-$H_{aliphatic}$), 1662 ν(C=O), 1608 ν(CH=$N_{azomethine}$), 1474 ν(N=N), 1261 ν(C-$O_{phenolic}$), 1122, 1006, 733, 690. UV–Vis (λ_{max}, nm): 502, 462, 365, 285, 265, 220. ^{1}H NMR (300 MHz, DMSO-d_6): δ = 9.58 (s, 1H), 8.74 (s, 1H), 8.11 (s, 1H, Ar-H), 7.87–7.84 (m, 4H, Ar-H), 7.63–7.31 ppm (m, 13H, Ar-H), 3.96 (s, 3H, OCH_3) ppm. ^{13}C NMR (75 MHz, DMSO-d_6): δ = 191.6, 170.5, 162.5, 151.9, 151.3, 149.7, 148.9, 143.8, 129.7, 129.4, 128.6, 128.2, 122.2, 118.4, 118.1, 115.6, 105.2, 56 ppm. ESI-MS (m/z): 530.5 [M + H].

General Process for the Synthesis of Metal Complexes

A solution of the metal salt $M(CH_3COO)_2 \bullet xH_2O$ (0.5 mmol) [99.75 mg $Cu(CH_3COO)_2 \bullet H_2O$; 124.5 mg $Ni(CH_3COO)_2 \bullet 4H_2O$; 124.5 mg $Co(CH_3COO)_2 \bullet 4H_2O$; 122.5 mg $Mn(CH_3COO)_2 \bullet 4H_2O$; 112.5 mg $Pd(CH_3COO)_2$] in MeOH (25 mL) was added dropwise to a stirred solution of 5-benzoyl-1-((E)-(2-hydroxy-3-methoxy-5-((E)-phenyldiazenyl)benzylidene)amino)-4-phenylpyrimidin-2(1H)-one (HL) (1 mmol, 530 mg) in a mixture of MeOH/$CHCl_3$ 1:1 (30 mL, V:V) as solvent at room temperature (Scheme 2). The mixture was stirred and heated to reflux for 1 h at 80 °C and then concentrated in a rotary evaporator to a volume of approximately 15 mL. The precipitate obtained was filtered and washed with hot methanol and diethyl ether. The final solid was dried under vacuum at 80 °C overnight.

$[CuL_2] \bullet 2H_2O$

The amber product is soluble in dimethylsulfoxide, *N,N′*-dimethylformamide. Yield 76%; Mp: 214 °C.

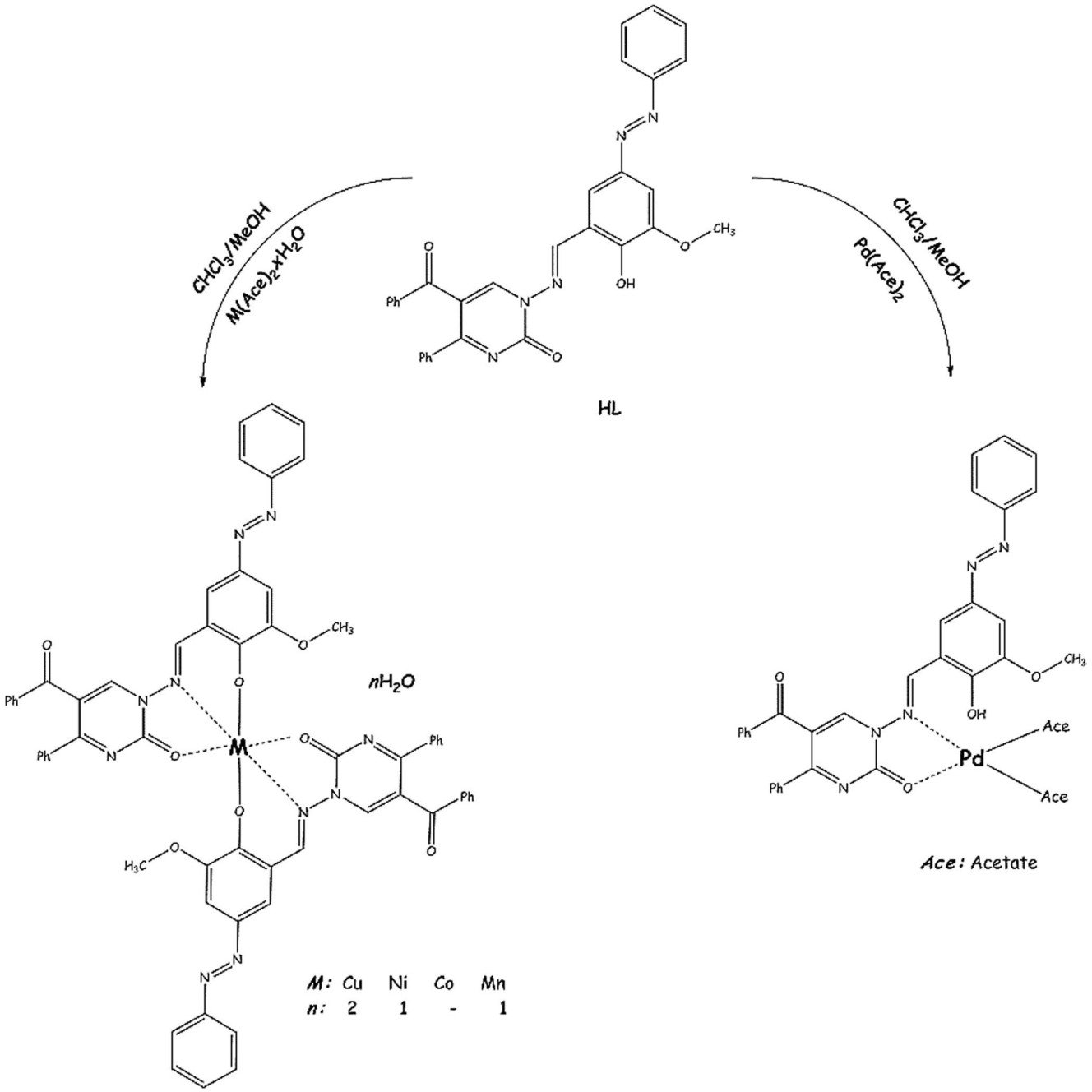

Scheme 2 Synthetic route and suggested possible structures of the metal complexes

Anal. Calc. for $C_{62}H_{50}CuN_{10}O_{11}$ (1156.65 g/mol): C, 64.39; H, 4.18; N, 12.11. Found: C, 64.36; H, 4.21; N, 12.04%. FTIR data (KBr, cm^{-1}): 3429 ν(OH/H_2O), 3059 ν(C-$H_{aromatic}$), 2831 ν(C-$H_{aliphatic}$), 1658 ν(C=O), 1604 ν(CH=$N_{azomethine}$), 1474 ν(N=N), 1251 ν(C-$O_{phenolic}$), 520 ν(Cu-O), 439 ν(Cu-N). UV–Vis (λ_{max}, nm): 511, 502, 438, 403, 285, 241, 216. μ_{eff}: 1.53 BM, Λo (S cm^2 mol^{-1}): 2.66. ESI-MS (m/z): 1060 [M-2H_2O-2CH_3O- + 2H].

[NiL_2]•H_2O

The dark blue product is soluble in dimethylsulfoxide, *N,N′*-dimethylformamide. Yield 56%; Mp: 283 °C. Anal. Calc. for $C_{62}H_{46}NiN_{10}O_9$ (1133.78 g/mol): C, 65.68; H, 4.09; N, 12.35. Found: C, 65.45; H, 4.08; N, 12.31%. FTIR data (KBr, cm^{-1}): 3448 ν(OH/H_2O), 3059 ν(C-$H_{aromatic}$), 2835 ν(C-$H_{aliphatic}$), 1654 ν(C=O), 1600 ν(CH=$N_{azomethine}$), 1477 ν(N=N), 1253 ν(C-$O_{phenolic}$), 513 ν(Ni-O), 416

ν(Ni-N). UV–Vis (λ_{max}, nm): 521, 422, 283, 264, 237. μ_{eff}, 2.67 BM, Λo (S cm^2 mol^{-1}): 2.34. ESI-MS (m/z): 1085 $[M\text{-}H_2O\text{-}2CH_3O^-]^{+3}$.

$[CoL_2]$

The dark blue product is soluble in dimethylsulfoxide, *N,N′*-dimethylformamide. Yield 52%; Mp: 262 °C. Anal. Calc. for $C_{62}H_{44}CoN_{10}O_8$ (1116.01 g/mol): C, 66.73; H, 3.97; N, 12.55. Found: C, 66.65; H, 3.87; N, 12.51%. FTIR data (KBr, cm^{-1}): 3059 ν($C\text{-}H_{aromatic}$), 2831 ν($C\text{-}H_{aliphatic}$), 1654 ν(C=O), 1597 ν($CH{=}N_{azomethine}$), 1477 ν(N=N), 1253 ν($C\text{-}O_{phenolic}$), 513 ν(Co-O), 451 ν(Co-N). UV–Vis (λ_{max}, nm): 515, 442, 264, 252, 218. μ_{eff}, 3.63 BM. Λo (S cm^2 mol^{-1}): 1.46. ESI-MS (m/z): 1113.95 $[M]^{+2}$.

$[MnL_2]\bullet H_2O$

The claret red product is soluble in dimethylsulfoxide, *N,N′*-dimethylformamide. Yield 79%; Mp: 277 °C. Anal. Calc. for $C_{62}H_{44}MnN_{10}O_8$ (1111.27 g/mol): C, 66.97; H, 3.99; N, 12.60. Found: C, 66.90; H, 3.92; N, 12.55%. FTIR data (KBr, cm^{-1}): 3445 ν(OH/H_2O), 3062 ν($C\text{-}H_{aromatic}$), 2920 ν($C\text{-}H_{aliphatic}$), 1600 ν($CH{=}N_{azomethine}$), 1477 ν(N=N), 1253 ν($C\text{-}O_{phenolic}$), 501 ν(Mn-O), 412 ν(Mn-N). UV–Vis (λ_{max}, nm): 514, 419, 284, 265. μ_{eff}, 6.01 BM. Λo (S cm^2 mol^{-1}): 3.19. ESI-MS (m/z): 1062$[M\text{-}H_2O\text{-}CH_3O^-]^{+2}$.

$[Pd(HL)(Ace)_2]$

The orange product is soluble in dimethylsulfoxide, *N,N′*-dimethylformamide. Yield 70%; Mp: 281 °C. Anal. Calc. for $C_{35}H_{29}PdN_5O_8$ (754.05 g/mol): C, 55.75; H, 3.88; N, 9.29. Found: C, 56.01; H, 3.90; N, 9.33%. FTIR data (KBr, cm^{-1}): 3055 ν($C\text{-}H_{aromatic}$), 2835 ν($C\text{-}H_{aliphatic}$), 1651 ν(C=O), 1604 ν($CH{=}N_{azomethine}$), 1473 ν(N=N), 1261 ν($C\text{-}O_{phenolic}$), 520 ν(Pd-O), 439 ν(Pd-N). UV–Vis (λ_{max}, nm): 400, 286, 264, 221, 211. μ_{eff}: D. Λo (S cm^2 mol^{-1}): 2.44. ESI-MS (m/z): 607 $[M\text{-}2CH_3COO^-\text{-}CH_3O^-]$.

Results and Discussion

The azo-azomethine ligand, HL, and its transition metal(II) complexes were prepared and characterized structurally as explained in the experimental section. All the derivatives are stable at room temperature and retained fine storage grade. The azo-azomethine ligand is soluble in common organic solvents such as EtOH, MeOH, THF, $CHCl_3$ while its transition metal(II) complexes are partially soluble in common organic solvents and well soluble in DMF and DMSO. The analytical and physical features of the complexes are dedicated in the experimental section.

Elemental Analysis

Elemental analysis indicates that the found and calculated values were within acceptable limits (±0.5). The elemental analysis data verifies that the composition of the complexes under interest is 1:2 metal:ligand stoichiometry and is in agreement with the suggested formula of $[ML_2]$ type for Cu(II), Ni(II), Co(II) and Mn(II) complexes and has the 1:1 metal:ligand stoichiometry [M(HL)] for Pd(II) complex (Scheme 2).

FT-IR Results

The bonding of the azo-azomethine ligand to the metal was investigated via the comparison of Fourier transform-infrared spectrum of the ligand with the spectra of the metal chelates. Useful data was obtained concerning the structure of the functional groups attached to the metal ions. The primary infrared bands and their definitions are presented in the experimental part. A strong band at 1608 cm^{-1} at the spectrum of the ligand in Fig. 1, can be referred to the -CH=N group. The shift of this band to a lower frequency due to a shift of lone pair density toward the metal ion, reveals the coordination of azomethine nitrogen to the metal center. The spectrum of the azo-azomethine ligand displays a broad band at 3433 cm^{-1} because of phenolic structure and water [29]. The FT-IR spectra of Cu(II), Ni(II) and Mn(II) metal chelates given in Fig. 1. They demonstrated broad bands at 3448 – 3429 cm^{-1} that belong to -OH group of the crystal water molecules in the structure of complex molecules (the presence of water was also verified by elemental and thermal analyses) [29, 30].

The carbonyl vibration of the pyrimidine ring at 1662 cm^{-1} shifted to 1658 – 1651 cm^{-1} after complexation, verifying the generation of a bond between the carbonyl oxygen and the metal. A comparison of infrared spectra of azo-azomethine based ligand and the metal(II) complexes also indicates that a band, characteristic of ν(C-O) at 1261 cm^{-1}, is shifted to 1253 – 1251 cm^{-1}, because of C-O-M bond formation [11]. Asymmetric and symmetric stretching vibrations of methyl group in the structure of the ligand were observed at 2970 – 2831 cm^{-1}. In addition, all the metal complexes reveal two new bands at 520 – 501 and 451 – 412 cm^{-1} which can be attributed to formation of M-O and M-N bonds, further verifying formation of coordination complexes [29]. However, the ν(C-O) band in the spectrum of the Pd(II) complex maintained at nearly the same value of 1261 cm^{-1}, proposing the C-O group does not take a part in complexation and showing bidentate coordination for the azo-azomethine ligand through the phenolic oxygen and nitrogen of the azomethine to the Pd (II) ion [3]. In the FT-IR spectrum of $[Pd(HL)(Ace)_2]$, the new carbonyl (C=O) stretch of the acetate ligand occurred at 1705 cm^{-1} (Fig. 1). In addition, the vibration band of the azo chromogen group both in the ligand and the complexes was observed at around 1474 cm^{-1}. Although the azo chromogen group has a donor character and

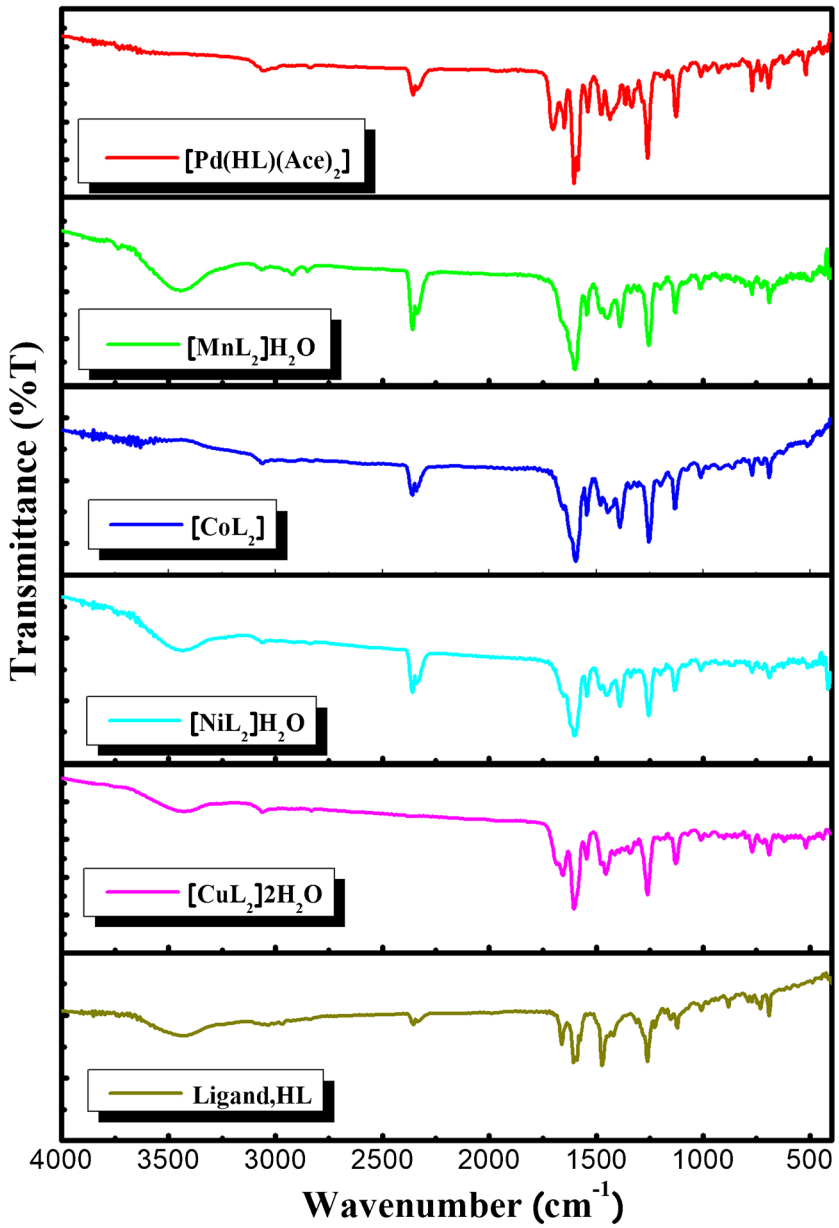

Fig. 1 FT-IR spectra of the azo-azomethine ligand and its transition metal (II) complexes

can form coordination compounds, the constant value of its vibration both in the ligand and the complexes shows that there is no coordination between the azo chromogen group and the metal ions [31]. All the vibrational data proposes that the metal ions are bonded to the azo-azomethine ligand through the phenolic oxygen, carbonyl oxygen of the pyrimidine ring and the imino nitrogen atoms.

NMR Spectroscopy

The ^{1}H and ^{13}C-NMR spectra of the ligand were taken at room temperature in deuterated dimethylsulfoxide solution ($(CD_3)_2S{=}O$) using TMS as an internal standard and the data are given in the experimental part. The ^{1}H-NMR spectrum of the ligand displays singlet signal in the 9.58 ppm which is attributed to the phenolic proton (-OH). Another singlet signal at 8.74 ppm is considered as the signal of the proton related to the azomethine group (-CH=N-) proton [7, 30]. The ^{1}H-NMR spectrum of the ligand demonstrates other signals at 8.11 (bs, 1H, Ar-H), 7.87–7.84 (m, 4H, Ar-H), 7.63–7.31 ppm (m, 13H, Ar–H) ppm for aromatic protons and 3.96 (s, 3H) for methoxy protons [7, 17]. Moreover, there is also water protons of the solvent ($(CD_3)_2S{=}O$), observed at 3.47 ppm [32]. The ^{13}C-NMR spectrum of the ligand (Fig. S1b) revealed characteristic signals at 191.6, 170.5, and 162.5 ppm because of (OC–Ar), (C=O, pyrimidine), and (−C6, pyrimidine ring) of the azo-azomethine base ligand, respectively. The peak at $\delta = 151.9$ ppm was due to azomethine carbon of the ligand. Additionally, the spectrum of the ligand displayed peaks between 151.3 and 105.2 ppm (151.3, 149.7, 148.9, 143.8, 129.7, 129.4, 128.6, 128.2, 122.2, 118.4,

118.1, 115.6 and 105.2 ppm) because of aromatic carbon atoms. Also, the peak at 56 ppm was due to aliphatic methoxy carbon [7, 30, 33].

Magnetic Susceptibility, Absorption Spectroscopy and Fluorescence Features

The general structural formula of the complexes are given in Scheme 2. It was specified that Cu(II), Ni(II), Co(II), and Mn(II) complexes are paramagnetic. The magnetic moment values (μ_{eff}) are in the 1.53–6.01 B.M. range for metal complexes at room temperature. Pd(II) complexes did not display any magnetism, as it was expected. All the compounds electronic absorption spectra were obtained in 10^{-3} M DMF solution between 200 and 800 nm at room temperature. In Table 1, the UV–Vis spectral data of the synthesized azo-azomethine ligand and its metal complexes are given. The electronic absorption spectra provide dependable knowledge concerning the ligand arrangement in transition metal complexes. The electronic spectra of the free ligand shows absorption bands at 220 and 265 nm, because of intraligand π-π* transitions and these bands remained nearly the same in the spectra of the complexes [26]. Absorptions in the 285 and 365 nm are attributed to the n-π* transition related to azomethine and the red shift of this absorption via complexation can be attributed to the donation of a lone pair of electrons to the metal ion, displaying the coordination of azomethine nitrogen of azo-azomethine ligand [33]. The band at 462 nm can be attributed to the transition within the molecule, actually an intramolecular charge transfer interaction [8, 33]. The Cu(II) complex exhibits a μ_{eff} value of 1.53 B.M., corresponding to one unpaired electron [34]. Ni(II) shows a magnetic moment of 2.67 BM, coherent with octahedral geometry [7–9]. Co(II) and Mn(II) complexes possess magnetic moments of 3.63 BM and 6.01 BM, which agree with values given for three unpaired electrons in an octahedral environment [35]. Moreover, the electronic spectra of the Cu(II), Ni(II), Co(II) and Mn(II) complexes demonstrated bands at 502, 511, 521, 515 and 514 nm, respectively. These bands are assigned to d-d transition in the complexes and are characteristics of octahedral complexes. The electronic spectra of the palladium(II) complex comprise intense bands at 476 and 400 nm, attributed to charge transfer and spin allowed transition for Pd(II) with a square planar stereochemistry [30, 33, 36].

Moreover, the absorption and emission properties of the azo-azomethine ligand and its complexes were investigated in freshly prepared solutions of toluene, ethylacetate and tetrahydrofuran (Figs. 2 and 3). The data obtained are given in Table 2.

Table 1 UV–Vis. (nm) data of the synthesized azo-azomethine ligand and its metal complexes in DMF

Compound	Absorption		λ_{max}(nm)	
	π–π*	n–π*	n-π*/CT	d–d
Ligand (HL)	220, 265	285, 365	462	–
$[CuL_2]\bullet 2H_2O$	216, 241	285	403, 438	502, 511
$[NiL_2]\bullet H_2O$	237	264, 283	422	521
$[CoL_2]$	218	264	442	515
$[MnL_2]\bullet H_2O$	265	284	419	514
$[Pd(HL)(Ace)_2]$	211, 221	264, 286	400	476

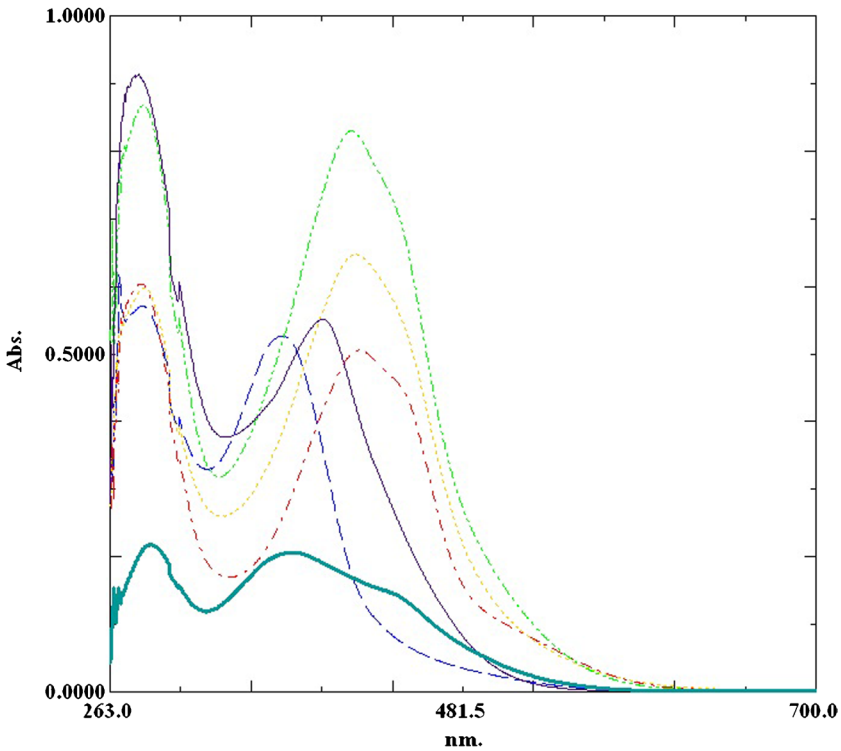

Fig. 2 Absorption spectra of the ligand (—) (1×10^{-5} M), $[CuL_2]\cdot 2H_2O$(– – –) ($0{,}9538\times10^{-5}$ M), $[CoL_2]$ (·····) ($0{,}9578\times10^{-5}$ M), $[NiL_2]\cdot H_2O$ (– · –) ($0{,}9591\times10^{-5}$ M), $[MnL_2]\cdot H_2O$ (– ·· –) ($0{,}9911\times10^{-5}$ M) and $[Pd(HL)(Ace)_2]$ (—) ($0{,}5880\times10^{-5}$ M) in ethylacetate

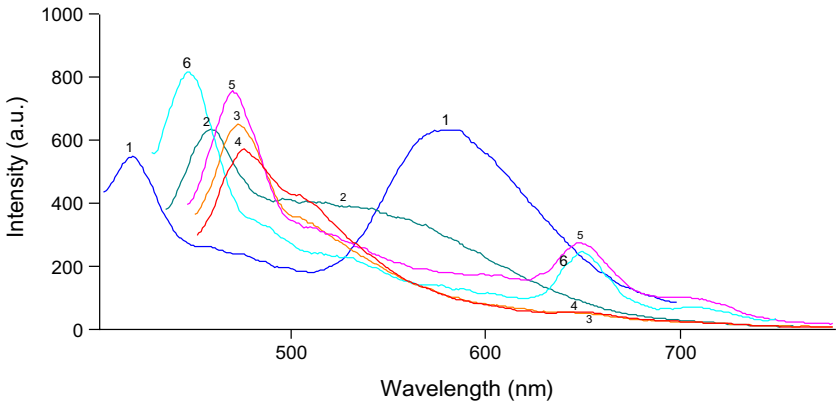

Fig. 3 Fluorescence spectra of the ligand (1) (1×10^{-5} M), $[CuL_2]\cdot2H_2O$ (2) ($0{,}9538\times10^{-5}$ M), $[CoL_2]$ (3) ($0{,}9578\times10^{-5}$ M), $[NiL_2]\cdot H_2O$ (4) ($0{,}9591\times10^{-5}$ M), $[MnL_2]\cdot H_2O$ (5) ($0{,}9911\times10^{-5}$ M) and $[Pd(HL)(Ace)_2]$ (6) ($0{,}5880\times10^{-5}$ M) in THF

Table 2 Absorption and emission maxima, λ (nm), molar extinction coefficients, ε (l $mol^{-1}cm^{-1}$), Stokes' shifts, Δλ (nm) and singlet energies, Es (kcal.mol^{-1}) of HL, $[CuL_2]\cdot2H_2O$, $[CoL_2]$, $[NiL_2]\cdot H_2O$, $[MnL_2]\cdot H_2O$ and $[Pd(HL)(Ace)_2]$ in toluene, tetrahydrofuran and ethyl acetate

Compound	Solvent	$\lambda^{abs}{}_{max}{}^{1}$	$\lambda^{abs}{}_{max}{}^{2}$	$\varepsilon_{max}{}^{1}$	$\varepsilon_{max}{}^{2}$	$\lambda^{ems}{}_{,max}{}^{1}$	$\lambda^{ems}{}_{,max}{}^{2}$	Δλ	Es^1	Es^2
HL	Toluene	286	367	19,000	20,700	421	575	54	67.7	49.6
	Tetrahydrofuran	283	373	27,180	22,800	419	585	46	68.2	48.7
	Ethylacetate	288	375	21,770	20,650	422	567	47	67.6	50.3
$[CuL_2]\cdot2H_2O$	Toluene	284	387	124,764	75,152	459	652	72	62.1	43.7
	Tetrahydrofuran	285	397	66,419	59,750	459	514	62	62.1	55.5
	Ethylacetate	283	370	25,425	26,442	414	730	44	68.9	39.0
$[CoL_2]$	Toluene	287	414	79,338	43,224	474	651	60	60.1	43.8
	Tetrahydrofuran	277	418	149,593	65,556	473	503	55	60.3	56.7
	Ethylacetate	285	415	62,341	67,582	474	647	59	60.1	44.0
$[NiL_2]\cdot H_2O$	Toluene	290	420	34,929	36,962	477	651	57	59.8	43.8
	Tetrahydrofuran	277	420	103,138	46,825	476	504	56	59.9	56.6
	Ethylacetate	282	417	62,788	52,716	475	651	58	60.0	43.8
$[MnL_2]\cdot H_2O$	Toluene	290	365	53,890	70,629	471	649	106	60.5	43.9
	Tetrahydrofuran	280	363	154,374	61,548	470	648	107	60.7	44.0
	Ethylacetate	284	413	87,519	83,715	472	651	59	60.4	43.8
$[Pd(HL)(Ace)_2]$	Toluene	287	400	86,684	76,446	447	650	47	63.8	43.8
	Tetrahydrofuran	278	399	261,905	87,415	447	649	48	63.8	43.9
	Ethylacetate	281	395	95,646	87,772	446	784	51	63.9	36.3

The azo-azomethine ligand and its complexes with Cu(II), Co(II), Ni(II), Mn(II) and Pd(II) have two absorption maxima in all the solvents studied; the first one is between 277 and 290 nm and the second one is between 365 and 420 nm, designated as π→π* and n→π* transitions, respectively (Table 2). The first absorption maxima of the azo-azomethine ligand and its transition metal (II) complexes are in the same region, but the second absorption maxima of transition metal(II) complexes are red shifted in comparison to the azo-azomethine ligand, and the biggest red shift was obtained for its $[NiL_2]\bullet H_2O$ complex.

The molar extinction coefficients of the complexes are higher than the molar extinction coefficients of azo-azomethine ligand. This is because the complexation of the ligands to metal ion increases their rigidity and thus reduces the loss of energy by thermal vibration decay. All the compounds displayed two emission maxima; the first one between 419 and 476 nm and the second one between 503 and 784 nm (Table 2). In general both the first and second emission maxima of the Cu(II), Co(II), Ni(II), Mn(II) and Pd(II) complexes is red shifted in comparison to the azo-azomethine ligand. The longest emission maxima was obtained for Pd(II) complex in ethylacetate. The compounds exhibited moderate Stokes' shift values ranging from 44 to 107 nm, which confers to the advantage of better spectral resolution in emission based studies. The biggest Stokes' shift value was observed for Mn(II) complex in tetrahydrofuran.

The photostabilities of the compounds in toluene, tetrahydrofuran and ethylacetate were identified with a steady-state spectrofluorimeter in time-based mode. Considering the data collected after 1 h, there was no considerable change in the fluorescence intensities of the compounds (Fig. 4).

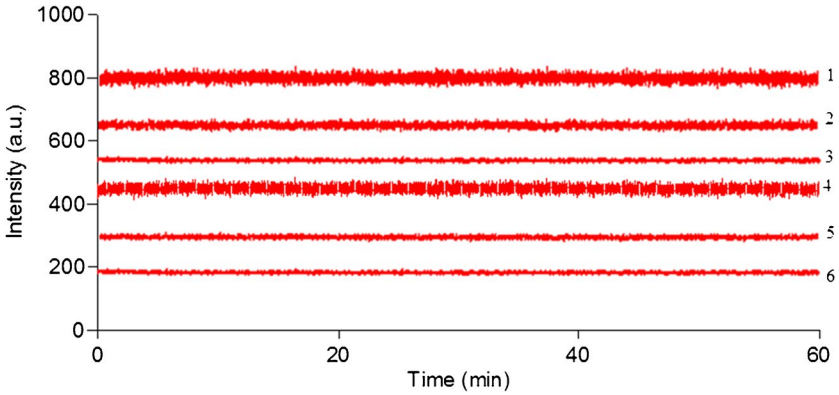

Fig. 4 Photostability test results of the ligand (1), $[CuL_2]\cdot 2H_2O$ (2), $[MnL_2]\cdot H_2O$ (3), $[Pd(HL)(Ace)_2]$ (4), $[NiL_2]\cdot H_2O$ (5) and $[CoL_2]$ (6) in THF after 1 h of monitoring

Molar Conductance

The molar conductance data of the transition metal(II) complexes obtained in 0.001 M solutions of DMF are shown in the experimental part. The data vary between 1.46 and 3.19 Ω^{-1} cm^2 mol^{-1}, which is the expected range for the complexes to behave as non-electrolytes [37].

Mass Spectroscopy

Mass spectra of synthesized compounds provides an important clue for elucidating the structure of azo-azomethine ligand and its transition metal(II) complexes. The mass spectra of the azo-azomethine ligand and its transition metal(II) complexes recorded at room temperature were used to compare their stoichiometry (Table 3).

Each synthesized compound was consistent with the molecular ion fragment and support the proposed structure of the complexes (Schemes 1 and 2). The spectra of the azo-azomethine ligand and its Co(II) complex are shown in the Supplementary data (Fig. S3(a–b)).

Thermal Analysis

The analyses were taken to examine the nature of the water molecules in the complexes and their thermal stabilities. In general, two kinds of water molecules are associated with the complexes which are lattice water and coordinated water. The lattice water is lost at low temperature (60–120 °C), whereas the coordinated water molecule is lost at high temperatures (150–200 °C) [38]. On heating, mass losses corresponded to H_2O, Ph–CO–, and the other organic moieties in the first, second, third, fourth, and fifth stages of decomposition. The Cu(II), Ni(II) and Mn(II) complexes suffered loss of H_2O in the first stage, the complexes contained 2, 1 and 1 moles of water of crystallization per complex molecule, respectively. The thermogram of the complexes of Co(II) and Pd(II) did not display any peak below 200 °C which revealed that there was no water molecule inside or outside the coordination sphere. The thermogravimetric curves of the $[CuL_2]\bullet 2H_2O$ and $[NiL_2]\bullet H_2O$ complexes are shown in Supplementary data (Figure S2).

Biological Applications

Antioxidant Activity

DPPH Radical Scavenging Ability The application of the DPPH process provides a simple and rapid way to measure antioxidants by spectrophotometry. The compounds free radical scavenging ability is presented in Fig. 5. In the presence of 10, 25, 50, 100, 200 and 500 mg/L, all tested compounds demonstrated nearly the same radical scavenging ability. The DPPH scavenging effect increased with the increasing concentrations of the compounds studied. At concentration of 5 mg/L, $Pd(HL)(Ace)_2$ demonstrated higher free

Table 3 Mass spectral data of the azo-azomethine ligand and its metal complexes

Compound	Calculated mass	Obtained mass m/z	Peak assigned
Ligand (HL)	529.55	530.5	[M + H]
$[CuL_2]\cdot 2H_2O$	1156.65	1060	$[M\text{-}2H_2O\text{-}2CH_3O^- + 2H]$
$[NiL_2]\cdot H_2O$	1133.78	1085	$[M\text{-}H_2O\text{-}2CH_3O^-]^{+3}$
$[CoL_2]$	1116.01	1113.95	$[M]^{+2}$
$[MnL_2]\cdot H_2O$	1111.27	1062	$[M\text{-}H_2O\text{-}CH_3O^-]^{+2}$
$[Pd(HL)(Ace)_2]$	754.05	574	$[M\text{-}2CH_3COO^-\text{-}2CH_3O^-]$

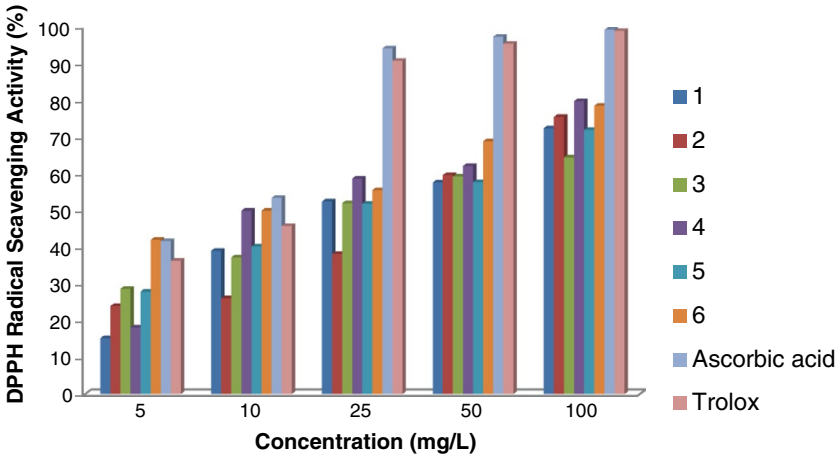

Fig. 5 Free radical scavenging abilities of the ligand (HL) (1); $[CoL_2]$ (2); $[CuL_2]\bullet 2H_2O$ (3); $[MnL_2]\bullet H_2O$ (4); $[NiL_2]\bullet H_2O$ (5); $[Pd(HL)(Ace)_2]$ (6)

radical scavenging ability than Ascorbic Acid and Trolox. The free radical scavenging ability was in the following order $[MnL_2]\bullet H_2O$ > $[Pd(HL)(Ace)_2]$ > $[CoL_2]$ > HL > $[NiL_2]\bullet H_2O$ > $[CuL_2]\bullet 2H_2O$ at 100 mg/L.

Ferrous Chelating Activity Fe^{2+} initiates free radicals through the Fenton and Haber–Weiss reaction. Fenton Weiss reaction is a reaction between Fe^{2+} and H_2O_2 which generates extremely reactive •OH implicated in various illnesses [39]. Percentage of Fe^{2+} chelating activity was demonstrated in Fig. 6. All tested compounds were able to chelate Fe^{2+} ions. Metal chelating activities of the compounds were found to be concentration dependent and linearly raised up with the compound concentration rise. When the concentration of HL, CoL_2, $[CuL_2]\bullet 2H_2O$, $[MnL_2]\bullet H_2O$, $[NiL_2]\bullet H_2O$, and $[Pd(HL)(Ace)_2]$ increased from 25 to 100 mg/mL, the chelating activities increased from 21.3 to 68.8%, from 11.1 to 29.7%, from 25.2 to 69.7%, from 48.6 to 87.5%, from 49.7 to 93.3%, and from 11.9 to 36.1%, respectively. As seen in Fig. 6, the compounds HL and $[CuL_2]\bullet 2H_2O$ showed significant chelating activity while compound $[MnL_2]\bullet H_2O$ and $[NiL_2]\bullet H_2O$ showed extremely significant chelating activity with standard substance EDTA.

Reducing Power The reducing power has been applied as one of the antioxidant ability indicators [40]. The existence of reductants in the studied compounds causes the reduction of the Fe^{3+}/ferricyanide complex to the ferrous form (Fe^{2+}) in the reducing power process. The quantity of Fe^{2+} complex can therefore be observed by measuring the formation of Perl's Prussian Blue at 700 nm [41]. Figure 7 indicates the reducing power of the compounds. The experimental results exhibited that the reducing power was dependent on concentration. Especially, the reducing power of $[NiL_2]\bullet H_2O$ and $Pd(HL)(Ace)_2$ were strong and raised steadily with rising concentrations of them. The reductive capability of tested compounds and Alpha-Tocopherol (AT) exhibited the following order: AT > $[NiL_2]\bullet H_2O$ > $[Pd(HL)(Ace)_2]$ > $[MnL_2]\bullet H_2O$ > $[CuL_2]\bullet 2H_2O$ > HL > $[CoL_2]$. As a result, these newly synthesized compounds were good electron and hydrogen donors and could finish the radical series reaction, turning free radicals into more harmless

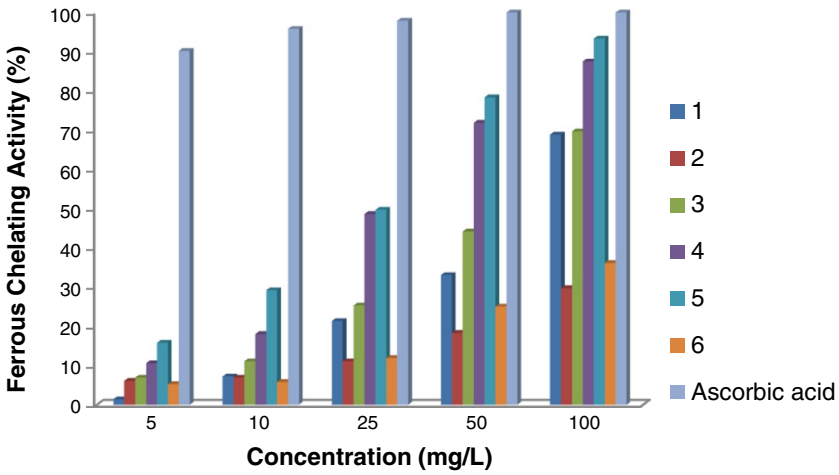

Fig. 6 Iron(II) chelating abilities of the ligand (HL) (1); $[CoL_2]$ (2); $[CuL_2]\bullet 2H_2O$ (3); $[MnL_2]\bullet H_2O$ (4); $[NiL_2]\bullet H_2O$ (5); $[Pd(HL)(Ace)_2]$ (6)

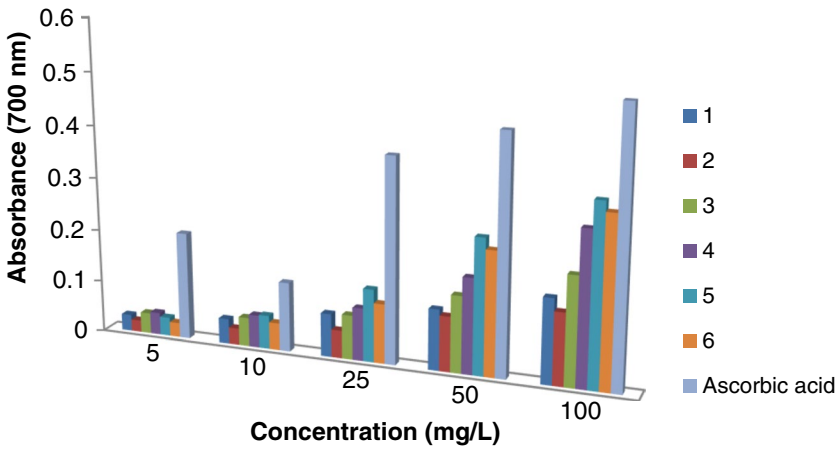

Fig. 7 Reducing power abilities of the ligand (HL) (1); $[CoL_2]$ (2); $[CuL_2]\bullet 2H_2O$ (3); $[MnL_2]\bullet H_2O$ (4); $[NiL_2]\bullet H_2O$ (5); $[Pd(HL)(Ace)_2]$ (6)

products. Our results based on the DPPH scavenging activity, ferrous chelating activity and reducing power of compounds recommended that they were likely to contribute significantly towards the antioxidant effect.

DNA Cleavage Studies

It is well known that, when pBR 322 plasmid DNA is exposed to gel electrophoresis to assess the quantity of strand cleavage, Form I displays the fastest running compared to Form II and Form III. If one strand is cut, Form I will relax to produce a slower moving nicked Form II. If both strands are cut, Form III is generated between the positions of Form I and Form II [42, 43]. The results of DNA cleavage abilities of ligand and its metal complexes are represented in Fig. 8. As seen in Lane 1, control study using pBR 322 plasmid DNA alone does not demonstrate a cleavage during the cleavage process. On the other hand, all tested compounds showed two strand DNA cleaving properties. These compounds can be used as anticancer drugs after various anticancer and toxicity test systems.

Antibacterial Activity

The synthesized compounds were examined for antimicrobial activity by using disc diffusion process. All tested compounds did not exhibit any antimicrobial activity to *Staphylococcus aureus* (ATCC 6538), *Legionella pneumophila* subsp. *pneumophiia* (ATCC 33152), *Bacillus subtilis* (6051), and *Candida albicans*. However, all test compounds showed moderate antibacterial activity (zone inhibition diameter ranging from 14 to 17 mm) against to *Bacillus cereus*. Also, ligand (HL) and its CoL_2, $[CuL_2]\bullet 2H_2O$, and $[NiL_2]\bullet H_2O$ complexes exhibited moderate antibacterial activity to *E. coli* (ATCC 10536) in 15, 14 and 18 zone inhibition diameter, respectively. Finally, ligand (HL), CoL_2, $[CuL_2]\bullet 2H_2O$ and $[MnL_2]\bullet H_2O$ compounds demonstrated moderate antibacterial activity 14, 17 and 19 mm against *E. hirae* (ATCC 10541), respectively.

Conclusion

The novel azo-azomethine ligand, was synthesized by condensation of *N*-aminopyrimidine-2-one with 2-hydroxy-3-methoxy-5-(phenyldiazenyl)benzaldehyde. The reactions of the azo-azomethine ligand with Cu(II), Ni(II), Co(II), Mn(II) and Pd(II) metal acetates yielded colored complexes. The synthesized compounds have been defined on the basis of Elemental analysis, FT-IR, ^{1}H NMR, ^{13}C NMR, UV–Vis, MS and thermal analysis (TGA/DTA) as well as the magnetic susceptibility and molar conductivity measurements indicating ONO tridentate donors. Due to physicochemical and spectroscopic results given above, the complexes may be

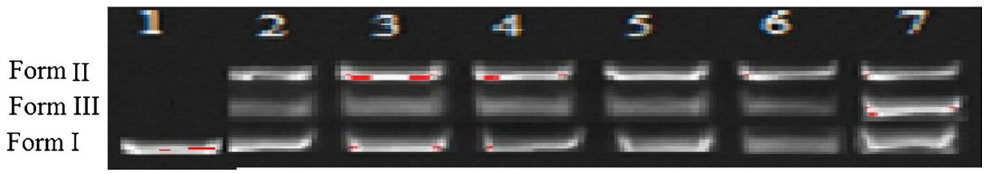

Fig. 8 The DNA cleavage pattern of pBR 322 DNA by newly synthesized of compounds. Lane 1, pBR 322 DNA; Lane 2, pBR 322 DNA + 50 µg/mL of HL; Lane 3, pBR 322 DNA + 50 µg/mL of $[CoL_2]$; Lane 4, pBR 322 DNA + 50 µg/mL of $[CuL_2]\bullet 2H_2O$; Lane 5, pBR 322 DNA + 50 µg/mL of $[MnL_2]\bullet H_2O$; Lane 6, pBR 322 DNA + 50 µg/mL of $[NiL_2]\bullet H_2O$; Lane 7, pBR 322 DNA + 50 µg/mL of $[Pd(HL)(Ace)_2]$

proposed to have octahedral geometry around Cu(II), Ni(II), Co(II) and Mn(II) complexes, and square planar geometry for Pd(II) complex. All the synthesized metal complexes were determined to be mononuclear. Furthermore, the investigation of absorption and emission properties of the azo-azomethine ligand and its corresponding metal complexes were evaluated in different solvents. The compounds dissipated moderate Stokes' shift values between 44 and 107 nm, which provides the benefit of better spectral resolution in emission related investigations. All derivatives exhibited excellent photostability in tetrahydrofuran, ethylacetate and toluene. The free radical scavenging features of prepared derivatives were interpreted by application of different methods, like the DPPH• scavenging activity, the metal chelating assay along with the reducing power. In addition, antimicrobial and pBR 322 plasmid DNA cleavage activities were investigated. All compounds showed good DPPH• scavenging activity and $[MnL_2]\bullet H_2O$ and $[NiL_2]\bullet H_2O$ compounds exhibited excellent metal chelating activity. All tested compounds demonstrated two strand DNA cleavage activities. The results of the present study reveals that these derivatives are especially powerful scavengers of free radicals and chelating agents. They can also exhibit DNA cleavage activities. However, further studies are needed to identify the compounds' toxic effects on living organisms and to develop their applications as food or drugs.

Acknowledgements This work was supported by University of Van Yüzüncü Yıl [FYL-2016-5334].

References

1. Schiff H (1864) Mitteilungen aus dem universitatslaboratorium in Pisa: Eineneue reihe organischer basen. Justus Liebigs Ann Chem 131:118–119
2. Abdel-Nasser MA, Alaghaz YA, Ammar HA, Bayoumi A, Sharah A (2014) Synthesis, spectral characterization, thermal analysis, molecular modeling and antimicrobial activity of new potentially N2O2 azo-dye Schiff base complexes. J Mol Struct 1074:359–375
3. Gulcan M, Sönmez M, Berber İ (2012) Synthesis, characterization, and antimicrobial activity of a new pyrimidine Schiff base and its Cu(II), Ni(II), Co(II), Pt(II), and Pd(II) complexes. Turk J Chem 36:189–200
4. Alghool S, Abd El-Halim HF, Dahshan A (2010) Synthesis, spectroscopic thermal and biological activity studies on azo-containing Schiff base dye and its cobalt(II), chromium(III) and strontium(II) complexes. J Mol Struct 983:32–38
5. Sönmez M, Çelebi M, Yardım Y, Sentürk Z (2010) Palladium(II) and platinum(II) complexes of a symmetric Schiff base derived from 2,6,diformyl-4-methylphenol with N-aminopyrimidine: synthesis, characterization and detection of DNA interaction by voltammetry. Eur J Med Chem 45:4215–4220
6. Borisova NE, Reshetova MD, Ustynyuk YA (2007) Metal-free methods in the synthesis of macrocyclic Schiff bases. Chem Rev 107:46–79
7. Anupama B, Sunita M, Shiva Leela D, Ushaiah B, Kumari CG (2014) Synthesis, spectral characterization, DNA binding studies and antimicrobial activity of Co(II), Ni(II), Zn(II), Fe(III) and VO(IV) complexes with 4-aminoantipyrine Schiff base of orthovanillin. J Fluoresc 24:1067–1076
8. Bitmez Ş, Sayin K, Avar B, Köse M, Kayraldız A, Kurtoglu M (2014) Preparation, spectral, X-ray powder diffraction and computational studies and genotoxic properties of new azo–azomethine metal chelates. J Mol Struct 1076:213–226
9. Anitha C, Sheela CD, Tharmaraj P, Sumathi S (2012) Spectroscopic studies and biological evaluation of some transition metal complexes of azo Schiff-base ligand derived from (1-phenyl-2,3-dimethyl-4-aminopyrazol-5-one) and 5-((4-chlorophenyl)diazenyl)-2-hydroxybenzaldehyde. Spectrochim Acta A 96:493–500
10. Marmion DM (1991) Handbook of U.S. colorants. 3rd ed. Wiley, New York
11. Bal M, Ceyhan G, Avar B, Köse M, Kayraldız A, Kurtoglu M (2014) Synthesis and X-ray powder difraction, electrochemical, and genotoxic properties of a new azo-Schiff base and its metal complexes. Turk J Chem 38:222–241
12. Kamel M, Galil F, Abdelwahab L, Osman A (1971) Some relations between chemical structure and light fastness of monoazo dispersed dyes. J Prakt Chem 313:1011–1021
13. Gopal J, Srinivasan M (1986) Preparation and properties of polyazo Schiff-bases. J Polym Sci Polym Chem Ed 24:2789–2796
14. Wang H, Song N, Li H, Li Y, Li X (2005) Synthesis and characterization of a partial-conjugated hyperbranched poly(p-phenylene vinylene) (HPPV). Synth Met 151:279–284
15. Gulcan M, Zengin H, Çelebi M, Sönmez M, Berber İ (2013) 2,6-Bis((E)-((5-benzoyl-2-thioxo-4-phenylpyrimidin-1(2 H)-yl) imino)methyl)-4-(methyl)phenol and its metal(II) complexes: synthesis, spectroscopy, biological activity, and photoluminescence features. Z Anorg Allg Chem 639:2282–2289
16. Gulcan M, Doğru Ü, Öztürk G, Levent A, Akbaş E (2014) Fluorescence properties and electrochemical behavior of some Schiff bases derived from N-aminopyrimidine. J Fluoresc 24:389–396
17. Gulcan M, Karataş Y, Işık S, Öztürk G, Akbaş E, Şahin E (2014) Transition metal(II) complexes of a novel symmetrical benzothiazole-based ligand: synthesis, spectral/structural characterization and fluorescence properties. J Fluoresc 24:1679–1686
18. Carrard M, Goncalves-Conto S, Si-Ahmed L, Ades D, Siove A (1999) Improved stability of interfaces in organic light emitting diodes with high Tg materials and self-assembled monolayers. Thin Solid Films 352:189–194
19. Feng L, Chen Z (2005) Synthesis and photoluminescent properties of polymer containing perylene and fluorene units. Polymers 46:3952–3956
20. Fang Q, Tanimoto A, Yamamoto T (2005) Synthesis and chemical properties of new photoluminescent poly(p-phenyleneethynylene) containing an electron-accepting benzothiadiazole unit and an electron-donating dialkoxybenzene unit: effect of twisting of the main chain on photoluminescence. Synth Met 150:73–78
21. Qin C, Wang X, Wang E, Hu C, Xu L (2004) Synthesis and characterization of a novel three-dimensional photoluminescent coordination polymer generated from unsymmetrically bridging ligand. Inorg Chim Acta 12:3683–3688
22. Heller A, Wasserman E (1965) Intermolecular energy transfer from excited organic compounds to rare-earth ions in dilute solutions. J Chem Phys 42:949–956
23. Prakash CR, Raja S, Saravanan G, Kumar PD, Selvam TP (2011) Synthesis and evaluation of antioxidant activities of some novel isatin derivatives and analogs. Asian J Res Pharm Sci 1:140–143
24. Dar AM, Manzoor S, Gatoo A (2015) Synthesis of new steroidal imidazo [1,2-a] pyridines: DNA binding studies, cleavage activity and in vitro cytotoxicity. Steroids 104:163–175
25. Chai CLL, Armarego WLF (2009) Purification of laboratory chemicals. Sixth ed. Elsevier, Oxford

26. Lever ABP (1984) Inorganic electronic spectroscopy. Elsevier, Amsterdam
27. Cabir B, Avar B, Gülcan M, Kayraldız A, Kurtoglu M (2013) Synthesis, spectroscopic characterization, and genotoxicity of a new group of azo-oxime metal chelates. Turk J Chem 37:422–438
28. Altural B, Akçamur Y, Sarıpınar E, Yıldırım I, Kollenz G (1989) Reactions of cyclics oxalyl compounds, part 29 [1] a simple synthesis of functionalized 1 H-pyrimidines. Monatsh Chem 120:1015–1020
29. Nakamoto K (1997) Infrared and Raman spectra of inorganic and coordination compounds. Wiley, New York
30. Gulcan M, Sönmez M (2011) Synthesis and characterization of Cu(II), Ni(II), Co(II), Mn(II), and Cd(II) transition metal complexes of tridentate Schiff base derived from o-vanillin and N-aminopyrimidine-2-thione. Phosphorus Sulfur Silicon 186:1962–1971
31. Sarigul M, Deveci P, Kose M, Arslan U, Dagi HT, Kurtoglu M (2015) New tridentate azo–azomethines and their copper(II) complexes: synthesis, solvent effect on tautomerism, electrochemical and biological studies. J Mol Struct 1096:64–73
32. Gottlieb HE, Kotlyar V, Nudelman A (1997) NMR chemical shifts of common laboratory solvents as trace impurities. J Org Chem 62:7512–7515
33. Alaghaz AMA, Bayoumi HA, Ammar YA, Aldhlmani SA (2013) Synthesis, characterization, and antipathogenic studies of some transition metal complexes with N,O-chelating Schiff's base ligand incorporating azo and sulfonamide moieties. J Mol Struct 1035:383–399
34. Patil SA, Prabhakara CT, Halasangi BM, Toragalmath SS, Badami PS (2015) DNA cleavage, antibacterial, antifungal and anthelmintic studies of Co(II), Ni(II) and Cu(II) complexes of coumarin Schiff bases: synthesis and spectral approach. Spectrochim Acta A 137:641–651
35. Naik KHK, Selvaraj S, Naik N (2014) Metal complexes of ONO donor Schiff base ligand as a new class of bioactive compounds; synthesis, characterization and biological evolution. Spectrochim Acta A 131:599–605
36. Tas E, Kilic A, Durgun M, Kupecik L, Yilmaz İ, Arslan S (2010) Cu(II), Co(II), Ni(II), Mn(II), and Fe(II) metal complexes containing N,N′-(3,4-diaminobenzophenon)-3,5-But2-salicylaldimine ligand: synthesis, structural characterization, thermal properties, electrochemistry, and spectroelectrochemistry. Spectrochim Acta A 75:811–818
37. Geary WJ (1971) The use of conductivity measurements in organic solvents for the characterisation of coordination compounds. Coord Chem Rev 7:81–122
38. Nikolaev AV, Myachina LI, Logvinenko VA (1969) Thermographic study of the structures of some simple, mixed and binuclear chelates of EDTA. Therm Anal 2:779–791
39. Lloyd RV, Hanna PM, Mason RP (1997) The origin of the hydroxyl radical oxygen in the Fenton reaction. Free Radic Biol Med 22:885–888
40. Bhandari MR, Kawabata J (2004) Organic acid, phenolic content and antioxidant activity of wild yam (Dioscorea spp.) tubers of Nepal. Food Chem 88:163–168
41. Chung SK, Osawa T, Kawakishi S (1997) Hydroxyl radical scavenging effects of spices and scavengers from brown mustard (Brassica nigra). Biosci Biotech Biochem 61:118–123
42. Kumar H, Devaraji V, Prasath R, Jadhao M, Joshi R, Bhavana P, Ghosh SK (2015) Groove binding mediated structural modulation and DNA cleavage by quinoline appended chalcone derivative. Spectrochim Acta A 151:605–615
43. Parveen S, Arjmand F, Ahmad I (2014) Enantiomeric in vitro DNA binding, pBR322 DNA cleavage and molecular docking studies of chiral L- and D-ternary copper(II) complexes of histidine and picolinic acid. J Photochem Photobiol B 130:170–178